One-dimensional Simulation of Transmural Heterogeneity of Cardiac Cellular Electromechanics

Yunliang Zang[1], Ling Dai[1], Yu Zhang[2], Ling Xia[1]

[1]Department of Biomedical Engineering, Zhejiang University, Hangzhou, China
[2]Patent Examination Cooperation Center of SIPO, Haidian District, Beijing, China

Abstract

Cardiac tissue exhibits transmural heterogeneous electromechanical characteristics which are responsible for normal activation, repolarization, contraction and relaxation in healthy hearts. Under abnormal conditions such as myocardial ischemia (MI), the original heterogeneity will be disrupted and may cause the heart out of function. In this paper, a transmural heterogeneous cellular electromechanics model has been developed. We used the model to simulate and validate transmural heterogeneity of the electrical properties and mechanical properties. In addition, the developed model was also used to simulate ventricular electrocardiograms (ECG) under normal and ischemia conditions on the multi-cellular 1-D fiber model. The results showed that our model could reproduce many transmural heterogeneous electromechanical features of the heart, and were in good accordance with experimental observations. The ECG under normal and ischemia conditions were compared to demonstrate the importance of the precise transmural heterogeneity.

1. Introduction

Electrophysiological heterogeneity within the heart has long been recognized. Many studies have found smaller I_{ks} and larger I_{NaL} mainly contribute to longer action potential duration (APD) in the midmyocardial (M) cell. Besides, Xiong found transmural heterogeneity of Na^{2+}-Ca^{2+} exchange current [1]. Li and his group found a smaller I_{to1} in the endocardial (Endo) cell, while larger in the M and epicardial (Epi) cell [2]. The original transmural heterogeneity is very important for the heart to maintain its function. In abnormal conditions such as MI, the original heterogeneity will be disrupted and the heart will get out of function. In this study, we developed a transmural heterogeneous electromechanics model, through which we reproduced many cardiac electromechanical characteristics such as APD dispersion and rate dependence, intracellular Ca^{2+} concentrations, duration, latency to onset of contraction, the time to peak and so on. MI condition was simulated incorporating hyperkalemia, hypoxia and acidosis. This model was also integrated into multi-cellular 1-D fiber model to simulate electrocardiograms under control and MI. By comparison, we could establish the connections between changed ionic activities and the morphology of ECG after MI.

2. Methods

2.1. Cellular electromechanics model

Greenstein electrophysiological model and Rice myofilament model acted as the basis to construct transmural cellular electromechanics model [3-4]. In this model, I_{NaL} was incorporated and transmural distributed with the ratio of 1:2:1 for Epi, M and Endo cell current amplitude. I_{to1} and I_{CaL} was adjusted based on new experimental observations. The changes according to recent experimental data we took were shown in Table 1.

Table 1. Adjusted parameters for the transmural myocytes.

Conductivity	Epi	M	Endo	Ref
G_{Ks}	0.07	0.035	0.07	[5]
G_{K1}	3.69	2.73	3.28	[6]
G_{NaL}	0.0015	0.003	0.0015	[7]
K_{NaCa}	0.67	0.27	0.27	[1]
K_{SR}	2.5	1	1	[8]
Kv_{scale}	1.27	1.27	0.51	[2]

In this model, the buffering of the low-affinity, regulatory Ca-binding site on troponin in the Ca-handling system is controlled by the apparent Ca binding of the Rice myofilament model, which is shown below:

$$\frac{d[Ca^{2+}]_{cyto}}{dt} = \beta_{cyto}\begin{cases}\frac{-C_{SA}}{2V_{cyto}F}(I_{Ca,b}+I_{p(Ca)}-2I_{NaCa})- \\ \frac{V_{ss}}{V_{cyto}}J_{xfer}-J_{up}-\frac{d[HTRPNCa]}{dt} \\ \frac{dTrop_{Apparent}}{1000dt}\end{cases} \quad (1)$$

The detailed meanings of the symbols in this equation can refer to the work of Greenstein and Rice. Notice that $Trop_{Apparent}$ is from Rice model and the others are from the Greenstein model [3-4].

2.2. MI simulation

MI model was constructed by incorporating the effects of hyperkalemia (elevating $[K^+]_o$), acidosis (lowering the amplitude of I_{Na} and I_{CaL}), hypoxia (activating I_{Katp}, ATP sensitive potassium current). The formulation of I_{Katp} is shown below [9]:

$$I_{K(ATP)} = \gamma p_0 f_{ATP} f_M f_N f_T (V_m - E_K)$$

$$\gamma = \frac{g_{\max}}{A} \cdot \left(\frac{[K^+]_o}{[K^+]_{o,control}}\right)^n$$

$$f_{ATP} = \frac{1}{1 + ([ATP]_i / K_m)^H}$$

$$K_m = 35.8 + 17.9 \cdot [ADP]_i^{0.256}$$

$$H = 1.3 + 0.74 \cdot \exp(-0.09 \cdot [ADP]_i)$$

$$f_M = \frac{1}{1 + \frac{[Mg^{2+}]_i}{K_{h,Mg}}} \qquad (2)$$

$$K_{h,Mg} = \frac{0.65}{\sqrt{[K^+]_o} + 5} \cdot \exp\left(-\frac{2 \cdot 0.32F}{RT} V_m\right)$$

$$f_N = \frac{1}{1 + \left(\frac{[Na^+]_i}{K_{h,Na}}\right)^2}$$

$$K_{h,Na} = 25.9 \cdot \exp\left(-\frac{0.35F}{RT} V_m\right)$$

$$f_T = Q_{10}^{\frac{T - T_0}{10}}$$

A: the capacitive membrane area. $[ATP]_i$: the intracellular ATP concentration. $[ADP]_i$: the intracellular ADP concentration. $[Mg^{2+}]_i$: the intracellular Mg^{2+} concentration. Other meanings of the symbols in this equation could refer to the work of Ferrero [9].

2.3. ECG simulation

The theoretical fiber with the length of 1.64 cm is composed of 60 Endo cells, 45 M cells and 60 Epi cells. The diffusion coefficient is homogeneous throughout the fiber and is set to 0.001cm^2ms^{-1}.

To eliminate the stimulus and end effects, only cells 6 to 155 were taken into account to compute ECG. The extracellular unipolar potentials generated by the fiber can be computed using the transmembrane potential V_m as follow [10]:

$$\Phi_e(x', y', z') = \frac{a^2}{4} \int (-\nabla V_m) \cdot [\nabla \frac{1}{r}] dx$$
$$r = [(x - x')^2 + (y - y')^2 + (z - z')^2]^{1/2} \qquad (3)$$

3. Results

This model could reproduce many transmural electromechanical features nearly the same as experimental observations. From Figure 1. A, B and C, M and Epi cell action potentials display a prominent spike and dome configuration, but absent in Endo cell. M cell has the longest APD90 and its rate dependence of APD is more accentuated than that of both Epi and Endo cells. The Endo cell has a smaller APD90 than M cell but larger than Epi cell at various pacing frequencies, which is very important for the formation of upright T wave in the ECG. The results from simulation were compared with experimental observations [6] in Figure 1. D and proved the ability of the model to simulate electrophysiological features in control.

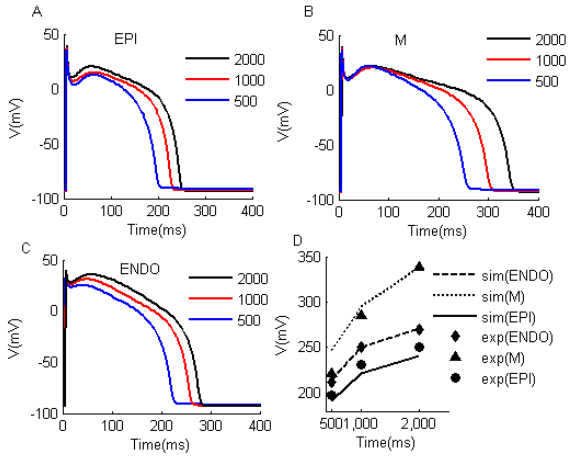

Figure 1. A: Epi cell AP morphology paced with CL =500, 1000 and 2000ms. B: M cell AP morphology paced with CL =500, 1000 and 2000ms. C: Endo cell AP morphology paced with CL =500, 1000 and 2000ms. D: APD adaptation from the model and experimental observations [6].

Figure 2 depicts the trace of simulated Ca2+ transients and active contraction. Intuitively, we could find the largest Ca2+ transient amplitude in the M cell from Figure 2. B. The Ca2+ duration from the Endo and M cell are bigger than that from the Epi cell. Endo cell latency to onset of contraction is 47 ms, larger than Epi (25 ms) and M cell (27 ms), which is a prerequisite for the ventricles to contract synchronously. From the simulation results,

the time to peak for Epi, M and Endo cell is 118ms ,177ms and 230 ms respectively. By comparing the simulation results with the experimental data from Cordeiro [11] in Table 2, we demonstrated the model could also satisfy the need to reproduce transmural mechanical characteristics.

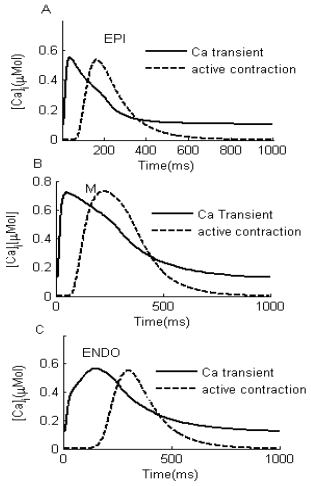

Figure 2. Ca^{2+} transients and active contraction.

Table 2. Simulated Ca^{2+} and active contraction properties compared with experiment measurements [11].

	Simulation/ Experiment		
	Latency	Time to peak	Ca^{2+} duration
Epi	25/28	118/104	327/494
M	27/29	177/172	604/732
ENDO	47/47	230/204	605/759

After acute MI, selective changes happen for the Epi, M and Endo cell. The presence of larger I_{to1} contributes to the loss of the plateau phase in the Epi and M cell. From the Figure 3, Endo cell Action potential underwent a relatively smaller depression than the M and Epi cell.

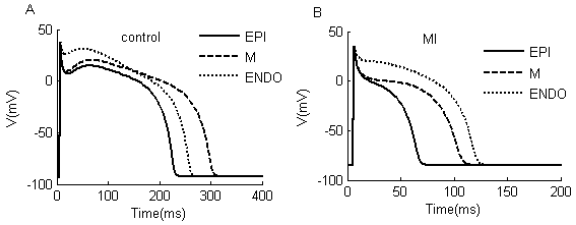

Figure 3. Simulated AP morphology after MI compared with control.

Using this transmural electrophysiological model, we simulated the ECG in control and MI. From Figure 4, we could find the simulated ECG is similar with experimental observations. It could recreate the QRS wave, J wave and upright T wave. For the reason of relatively small APD dispersion among Epi, M and Endo cells, the T wave was a little smaller than usually observed. MI made a depressed action on the APD and the larger I_{Katp}, I_{to1} shortened the APD in M and Epi cells much more than in Endo cell. As shown in the simulation results, shortened APD at the three parts at the same time shortened the QT-interval. However, due to the deficiency of the original model, MI made a much larger effect on the APD shortening than in reality. So the APD dispersion after MI was not as big as control which results in an even smaller T wave after MI in inconsistent with experimental observations.

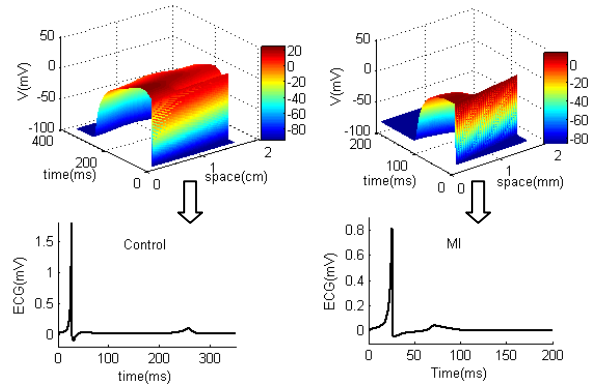

Figure 4. Simulated action potential propagation along the fiber together with the ECG in control and MI.

4. Discussion and conclusions

The developed transmural electromechanics model allows us to establish a platform to recreate electrophysiological and mechanical properties. By changing simulation condition and results, we could get a better understanding between the microscopic ionic process and the macroscopic phenomena. M cell has a longer APD for its larger I_{NaL}, I_{to1} and smaller I_{Ks}, I_{k1}. Specifically, larger I_{to1} makes a notch in the phase 1 of the action potential morphology and provides a larger driving force for I_{CaL} to lengthen the APD. For the Epi cell, although I_{to1} plays the same role as in the M cell, it could not compensate the role of larger I_{Ks}, I_{k1} and I_{NaCa} and its APD is even smaller than Endo cell. The simulated Ca^{2+} and mechanical properties are in good agreement with experimental observations. Many literatures have reported an EM delay among the different regions of the heart [12]. The latency to onset of contraction simulated in our work just supported that idea. From Table 2, the difference between Endo and Epi cell latency to onset of contraction is 22ms. And the time needed for the activation travelling from the endocardium to epicardium is on the order of 10 ms close to the above difference. So the original difference in the latency to onset of contraction is necessary for the ventricles to contract synchronously. Once disrupted, it will depress the heart's pump function.

Different parts of the heart will selectively change after MI as in our simulation. I_{Katp} is largest in the Epi cell, medium in the M cell and smallest in the Endo cell, which plays a main role for the changes after MI. Besides, Endo cell has a smaller I_{to1}, relatively high action potential plateau phase and is not susceptible to the harm from MI.

Although our model has proved its ability in many aspects of the simulation, it still has some limitations. First, for the reason of 40 Markov states, the coupled model composed of as many as 87 ordinary differential equations (ode) and it will take a long time to reach the steady state, which will be even worse in the 1-D, 2-D and 3-D simulations. Second, this ode system is much too stiff and is too crucial for the solver. Frequently used Runge-Kutta and Euler method is not appropriate for this model. We had to use another solver Radau5 to solve this equation [13]. Third, this model could not recreate the elevated T wave after MI. Besides, the myofilament model was developed for a rat model, so new experimental data for canine and humans are needed for future studies.

The model has been implemented in 1-D fiber model as a try and in the future it could be embedded into tissue electromechanics model so that it could serve as a tool for the physicians to optimize the therapy.

References

[1] Xiong W, Tian Y, DiSilvestre D, Tomasell GF. Transmural heterogeneity of Na+-Ca2+ exchange: evidence for differential expression in normal and failing hearts. Circ Res 2005; 97: 207-209.

[2] Li GR, Lau CP, Ducharme A, Tardif JC, Nattel S. Transmural action potential and ionic current remodeling in ventricles of failing canine hearts. Am J Physiol Heart Circ Physiol 2002; 283: H1031-1041.

[3] Greenstein JL, Hinch R, Winslow RL. Mechanisms of excitation-contraction coupling in an integrative model of the cardiac ventricular myocyte. Biophys J 2006; 90: 77-91.

[4] Rice JJ, Wang F, Bers DM, de Tombe PP. Approximate model of cooperative activation and crossbridge cycling in cardiac muscle using ordinary differential equations. Biophys J 2008; 95: 2368-2390.

[5] Liu DW, Antzelevitch C. Characteristics of the delayed rectifier current (IKr and IKs) in canine ventricular epicardial, midmyocardial, and endocardial myocytes. A weaker IKs contributes to the longer action potential of the M cell. Circ Res 1995; 76: 351-365.

[6] Liu D, Gintant G, Antzelevitch C. Ionic bases for electrophysiological distinctions among epicardial, midmyocardial, and endocardial myocytes from the free wall of the canine left ventricle. Circ Res 1993; 72: 671-687.

[7] Zygmunt AC, Eddlestone GT, Thomas GP, Nesterenko VV, Antzelevitch C. Larger late sodium conductance in M cells contributes to electrical heterogeneity in canine ventricle. Am J Physiol Heart Circ Physiol 2001; 281: H689-697.

[8] Laurita KR, Katra R, Wible B, Wan X, Koo MH. Transmural heterogeneity of calcium handling in canine. Circ Res 2003; 92: 668-675.

[9] Ferrero JM Jr, Saiz J, Ferrero JM, Thakor NV. Simulation of action potentials from metabolically impaired cardiac myocytes. Role of ATP-sensitive K+ current. Circ Res 1996; 79: 208-221.

[10] Plonsey R, Barr RC. Bioelectricity: A Quantitative Approach. 1988.

[11] Cordeiro JM, Greene L, Heilmann C, Antzelevitch D, Antzelevitch C. Transmural heterogeneity of calcium activity and mechanical function in the canine left ventricle. Am J Physiol Heart Circ Physiol 2004; 286: H1471-1479.

[12] Kerckhoffs RC, Faris OP, Bovendeerd PH, Prinzen FW, Smits K, McVeigh ER, Arts T. Electromechanics of paced left ventricle simulated by straightforward mathematical model: comparison with experiments. Am J Physiol Heart Circ Physiol 2005; 289: H1889-H1897.

[13] Hairer E, Wanner G. Stiff differential equations solved by Radau methods. J Comput Appl Math 1999; 111: 93-111.

Address for correspondence.

Name: Ling Xia
Full postal address: Department of Biomedical Engineering, Zhejiang University,
Hangzhou, China,
310027
E-mail address (optional): xialing@zju.edu.cn